Article

Discovery Medicine 2024; 36(183): 678–689
https://doi.org/10.24976/Discov.Med.202436183.64

Changes and Significance of Central Carbon Metabolism before and after Metformin Treatment of Type 2 Diabetes Based on Mass Spectrometry

Yang Shu[1,2,3,†], Fujie Yang[1,†], Weidong Li[1,2,3], Lisha Li[1], Qiongying Hu[1], Daqian Xiong[1,*]

[1]Department of Laboratory Medicine, Hospital of Chengdu University of Traditional Chinese Medicine, 610072 Chengdu, Sichuan, China
[2]College of Medical Technology, Chengdu University of Traditional Chinese Medicine, 610075 Chengdu, Sichuan, China
[3]Chongqing Key Laboratory of Sichuan-Chongqing Co-Construction for Diagnosis and Treatment of Infectious Diseases Integrated Traditional Chinese and Western Medicine, 400011 Chongqing, China
*Correspondence: 18981885710@163.com (Daqian Xiong)
[†]These authors contributed equally.
Published: 20 April 2024

Background: An imbalance in energy metabolism serves as a causal factor for type 2 diabetes (T2D). Although metformin has been known to ameliorate the overall energy metabolism imbalance, but the direct correlation between metformin and central carbon metabolism (CCM) has not been thoroughly investigated. In this study, we employed a high-performance ion chromatography-tandem mass spectrometry (HPIC-MS/MS) technique to examine the alterations and significance of CCM both before and after metformin treatment for T2D.

Methods: We recruited 29 participants, comprising 10 individuals recently diagnosed with T2D (T2D group). Among these, 10 patients underwent a 4–6-week treatment with metformin (MET group). Additionally, we included 9 healthy subjects (CON group). Employing HPIC-MS/MS, we quantitatively analyzed 56 metabolites across 18 biologically relevant metabolic pathways associated with CCM. Univariate and multivariate statistical analyses were utilized to identify differential metabolites. Subsequently, correlation analyses and Kyoto Encyclopedia of Genes and Genomes (KEGG) pathway analysis were conducted on the identified differential metabolites.

Results: We identified seven distinct metabolites in individuals with T2D ($p < 0.05$). Notably, cyclic 3′,5′-Adenosine MonoPhosphate (AMP), Glucose 6-phosphate, L-lactic acid, Maleic acid, and Malic acid exhibited a reversal to normal levels following metformin treatment. Furthermore, Malic acid demonstrated a positive correlation with L-lactic acid ($r = 0.94$, $p < 0.05$), as did succinic acid with malic acid ($r = 0.81$, $p < 0.05$), L-lactic acid with succinic acid ($r = 0.78$, $p < 0.05$), and L-lactic acid with glucose-6-phosphate ($r = 0.72$, $p < 0.05$). These metabolites were notably enriched in pyruvate metabolism ($p = 0.005$), tricarboxylic acid cycle (TCA) ($p = 0.007$), propanoate metabolism ($p = 0.007$), and glycolysis or gluconeogenesis ($p = 0.009$), respectively.

Conclusions: We employed HPIC-MS/MS to uncover alterations in CCM among individuals recently diagnosed with T2D before and after metformin treatment. The findings suggest that metformin may ameliorate the energy metabolism imbalance in T2D by reducing intermediates within the CCM pathway.

Keywords: type 2 diabetes: metformin; central carbon metabolism; HPIC-MS/MS; metabolites

Introduction

The global prevalence of diabetes is steadily increasing each year, with over 90% of patients diagnosed with type 2 diabetes (T2D), which is one of the major diseases threatening human health [1,2]. T2D, a chronic and progressive metabolic disease characterized by hyperglycemia [3], remains an incurable condition throughout an individual's life. Metformin (N, N-Dimethyl biguanide) stands as a primary oral medication for T2D treatment, endorsed by national guidelines worldwide as a monotherapy for newly diagnosed T2D patients [4–7]. Despite its clinical use for over 60 years, the precise mechanism of action of metformin remains incompletely understood. Recent research indicates that metformin disrupts glycolysis and oxidative phosphorylation [8–10], influencing Adenosine Triphosphate (ATP) production by activating AMP-activated protein kinase (AMPK) energy sensors [11–13]. The ATP production pathway is intricately connected to central carbon metabolism (CCM), encompassing traditional elements like glycolysis, the pentose phosphate pathway (PPP), and the tricarboxylic acid cycle (TCA). Additionally, CCM involves the breakdown of amino acids, lipids, and other substances, producing substrates that enter the TCA cycle to

participate in metabolic processes [14,15]. Nonetheless, the specific mechanisms through which metformin interferes with CCM remain less clear.

Metabolomics involves the comprehensive identification and quantification of all target metabolites, which are small molecules within the range of 50–1500 Daltons, in an organism under specific conditions or diseases [16]. It is categorized into non-targeted metabolomics and targeted metabolomics based on research objectives. Non-targeted metabolomics offers broad coverage of substances, allowing for the collection of extensive information on relative substance abundance [17]. In contrast, targeted metabolomics employs standard substances for different compounds to generate standard curves, facilitating the high-throughput detection of each metabolite in a specific pathway. It aims to establish relationships between substances through data analysis [17]. High-performance ion chromatography-tandem mass spectrometry (HPIC-MS/MS) serves as a targeted metabolomics assay characterized by high specificity, sensitivity, and repeatability [18,19]. Previous studies employing non-targeted metabolomics techniques have identified changes in metabolic profiles in T2D patients [20–24]. Carbohydrate and energy-related metabolites have been linked to a higher risk of T2D [24,25]. Additionally, research has indicated that metformin can influence energy metabolism in T2D patients [26–32], impacting glycolysis/gluconeogenesis, TCA, PPP, urea cycle, fatty acid metabolism, amino acid, and carnitine metabolism. However, compounds within the energy metabolic pathway have not been directly quantitatively analyzed. To further elucidate changes and significance in compounds related to CCM pathways in newly diagnosed T2D patients before and after metformin treatment, we utilized HPIC-MS/MS to quantitatively detect 56 metabolites across more than 18 potential CCM-related (biologically related) metabolic pathways. Through statistical analysis and the identification of differential metabolites, we delved into the clinical value and significance of these changes in the context of metformin treatment for T2D. This approach aims to provide a deeper understanding of the new mechanisms through which metformin improves energy metabolism.

Materials and Methods

Patient Recruitment and Study Design

Between October 2022 and May 2023, we recruited 10 newly diagnosed patients with type 2 diabetes admitted to the Department of Endocrinology at the Affiliated Hospital of Chengdu University of Traditional Chinese Medicine (T2D group). These patients were subsequently assigned to the metformin treatment group (MET group) and were prescribed metformin hydrochloride extended-release tablets (brand: Merck Seranogat, specification: 0.5 g × 20 tablets) for a period of 4–6 weeks. It is noteworthy that the patients receiving metformin treatment were the same individuals initially diagnosed with T2DM. As part of the treatment regimen, patients were instructed to take one tablet of metformin (0.5 g) at breakfast or within half an hour after a meal. They were advised to abstain from alcohol and smoking during this period, avoid overeating, and maintain their regular diet without any specific requirements.

Concurrently, 9 healthy subjects (CON group) were selected from the physical examination center of the Affiliated Hospital of Chengdu University of Traditional Chinese Medicine. The selection criteria ensured that their gender and age did not statistically differ from those of the newly diagnosed T2D patients. All recruited individuals met the early diagnosis criteria for T2D updated by the World Health Organization (WHO) in 2019 [33]. None of the participants had received any anti-diabetic drugs, including metformin. Exclusion criteria encompassed the individuals with cardiovascular disease, kidney disease, cancer, nerve injury, pregnancy, lactation, menstruation, and other major illnesses. Healthy subjects had no personal or family history of diabetes, exhibited normal fasting and 2-hour postprandial blood glucose levels, glycated hemoglobin, and islet function. They also did not present with dyslipidemia, cardiovascular diseases, or clinical symptoms of diabetes.

Our study, approved by the Clinical Research Ethics Committee of the Affiliated Hospital of Chengdu University of Traditional Chinese Medicine (2020KL-031), adhered to the principles of the 1964 Declaration of Helsinki and its subsequent amendments [34,35]. Informed consent was obtained from all eligible subjects who met the inclusion criteria.

Experimental Reagents and Instruments

The primary reagents employed in this experiment, including Methanol, Acetic acid, and Sodium Hydroxide, were of Liquid chromatograph-mass spectrometer (LC-MS) grade and sourced from CNW Technologies (Munich, Bavaria, Germany). It is important to note that in LC-MS analysis, only the target compound itself was subject to analysis, precluding the analysis of inorganic ions in its salt form. However, the hydrochloride, sodium salt, and ammonium salt of the target compound could be utilized as standards. The standard information for the 56 quantitative compounds is detailed in **Supplementary Files 1,2**.

The key instruments utilized in this experiment comprised ion chromatography ICS6000 (Thermo Scientific, Waltham, MA, USA), mass spectrometry 6500 QTrap+ (ABSciex, Framingham, MA, USA), centrifuge Heraeus Fresco17 (Fisher Scientific, Pittsburgh, PA, USA), ultrasonic instrument YM-080S (Fangao Microelectronics Co., Ltd, Shenzhen, China), grinding instrument JXFSTPRP-24 (Jingxin Technology Co., Ltd, Shanghai, China), and freezing centrifuge concentrator CV600 (Jiaimu Technology Co., Ltd, Beijing, China).

Serum Metabolite Extraction

Each volunteer underwent an 8-hour fasting period, and two tubes of whole blood were collected between 8–9 AM the following day. One tube, containing heparin as an anticoagulant, was subjected to testing for clinical biochemical markers. The other tube, containing serum without an anticoagulant, was separated and collected, with the serum stored in a refrigerator at –80 °C. Subsequent to the collection of all samples, HPIC-MS/MS detection was conducted.

For sample processing, the frozen samples were taken out of the –80 °C refrigerator and defrosted in an ice water bath. Following defrosting, the samples were vortex-mixed for 30 seconds. A precise 100 µL aliquot of each sample was transferred to an EP tube. Methanol (300 µL) was added to each sample, followed by vortex mixing for 30 seconds. The samples were then sonicated for 15 minutes in an ice-water bath, incubated at –40 °C for one hour, and centrifuged at 12,000 rpm (RCF = 13,800 (×g), R = 8.6 cm) and 4 °C for 15 minutes. A 320 µL aliquot of the supernatant was transferred to an EP tube, subjected to vacuum and spin drying, and subsequently re-dissolved with 160 µL pure water. The reconstituted samples were vortexed before being filtered through a filter membrane. Finally, the supernatant was transferred into an LC sample bottle for HPIC-MS/MS analysis.

HPIC-MS/MS Experimental Procedure

Serum samples underwent testing following established methods [36,37], encompassing the configuration of a standard solution, establishment of chromatographic and mass spectrometry conditions, determination of detection limit, quantitation limit, and evaluation of precision and accuracy of the method. Quality control (QC) samples for serum were generated by combining equal volumes of all samples to be tested, serving as a means to assess the repeatability of mass spectrometry results following identical treatment. During the analysis, two initial checks on the QC sample were performed, with subsequent checks conducted after every four samples, and a final check at the conclusion of the analysis, totaling ten repetitions.

The precision of this experimental method was assessed through the standard relative deviation (RSD) calculated from 10 repeated QC samples. Accuracy was gauged by the recovery rate of QC samples, calculated as (mean measured concentration) × (spiked concentration) $^{-1}$ × 100%. For HPIC- Multiple Reaction Monitoring (MRM)-MS analysis, the calibration solution was sequentially diluted by 2 times, and the lower limits of detection (LLOD) and the lower limits of quantitation (LLOQ) were determined based on signal-to-noise ratio. Following the guidelines of the US FDA for the validation of bioanalytical methods, the LLOD and LLOQ were defined as the concentrations of a compound corresponding to a signal-to-noise ratio of 3 and 10, respectively.

Data Processing and Analysis

Statistical analysis of patients' age, weight, body mass index (BMI), and biochemical test indicators was conducted using SPSS 26.0 (SPSS, Chicago, IL, USA). Measurement data were presented as mean ± standard deviation. If the three groups of data satisfied the conditions of normality and homogeneity of variance, a one-way analysis of variance and least significant difference (LSD)-t post hoc test were employed for comparisons. In cases where normality and homogeneity of variance assumptions were violated, the Kruskal-Wallis rank sum test was applied.

Mass spectrometry data acquisition and quantitative analysis of target compounds were executed using AB SCIEX Analyst Work Station Software (version 1.6.3, AB SCIEX, Boston, MA, USA), MultiQuant (version 3.0.3, AB SCIEX, Boston, MA, USA), and Chromeleon7 (version 7.1, Dionex, Sunnyvale, CA, USA). Raw data were preprocessed as follows [38]: (1) Filtration of individual metabolites; if a metabolite was missing in a single group >50%, it was conservatively excluded (**Supplementary File 3**). (2) Missing value recoding in the original data was performed using the numerical simulation method, where the minimum value was multiplied by a random number (0.1, 0.5) to fill in the gaps (**Supplementary File 4**).

After obtaining the quantitative expression matrix of all samples, the student *t*-test was applied for univariate statistical analysis, calculating the difference multiples. Additionally, principal component analysis (PCA) and orthogonal partial least squares discriminant analysis (OPLS-DA) were employed for multivariate statistical analysis. The utilization of both statistical methods facilitated a comprehensive observation of data, preventing false positive errors and overfitting of models that might arise from relying solely on one statistical method [39]. Furthermore, various online analysis tools and R software (version 4.1.0, Unversity of Auckland, Auckland, New Zealand) were utilized to visualize the data, incorporating tools such as Venn charts, volcano maps, correlation analyses, and Kyoto Encyclopedia of Genes and Genomes (KEGG) pathway analyses.

Results

Demographic Characteristics and Clinical Biochemical Indicators

Table 1 presents the results of demographic information and clinical biochemical indexes for the CON group, T2D group, and MET group after testing (refer to **Supplementary File 5** for the original data). No significant differences were observed in terms of sex, age, and BMI between the CON and T2D groups ($p > 0.05$), where BMI is calculated using the formula: weight (kg)/height (m)^2. In the realm of clinical biochemical indices, the T2D group exhibited significantly higher levels of Fasting plasma glucose (FBG) ($p = 0.000$), Glycated hemoglobin (HbA1c) ($p = 0.000$), and triglyceride (TG) ($p = 0.023$) compared

Table 1. Demographic Characteristics and clinical chemistry parameters.

Clinical parameters	Group			p_1	p_2	p_3	F	p
	T2D (n = 10)	CON (n = 9)	MET (n = 10)					
Gender (M/F)	3/7	3/6		0.541			0.389	0.541
Age (years)	43.7 ± 11.24	40.0 ± 13.84		0.529			0.413	0.529
BMI (kg/m^2)	23.75 ± 2.43	22.67 ± 3.18		0.415			0.697	0.415
FBG (mmol/L)	7.45 ± 1.19	4.96 ± 0.35	6.19 ± 1.60	0.000*	0.026*	0.032*	10.444	0.000*
HbA1c (%)	6.83 ± 0.96	5.01 ± 0.26	6.78 ± 0.94	0.000*	0.890	0.000*	15.479	0.000*
FINS (mIU/L)	20.05 ± 22.83	8.02 ± 0.98	18.65 ± 23.34	0.158	0.873	0.239	1.092	0.350
TC (mmol/L)	5.27 ± 1.63	4.21 ± 0.67	5.31 ± 1.55	0.108	0.940	0.094	1.900	0.170
TG (mmol/L)	2.57 ± 1.74	1.18 ± 0.59	2.05 ± 1.09	0.023*	0.058	0.145	2.947	0.070
HDL (mmol/L)	1.32 ± 0.77	1.26 ± 0.19	1.32 ± 0.71	0.841	1.000	0.841	0.027	0.973
LDL (mmol/L)	3.16 ± 1.18	2.50 ± 0.52	3.26 ± 1.33	0.202	0.830	0.141	1.332	0.281
BUN (mmol/L)	4.45 ± 1.64	4.83 ± 1.00	4.45 ± 1.84	0.597	1.000	0.597	0.188	0.830
CREA (mmol/L)	57.34 ± 11.14	66.27 ± 11.65	59.08 ± 12.96	0.116	0.747	0.202	1.463	0.250

Abbreviations: BMI, body mass index; FBG, Fasting plasma glucose; HbA1c, Glycated hemoglobin; FINS, Fasting serum insulin; TC, total cholesterol; TG, triglyceride; HDL, high-density lipoprotein; LDL, Low-density lipoprotein; BUN, blood urea nitrogen; CREA, Creatinine. Note: All parameters are mean ± SD, * indicates that the p-value is lower than 0.05. p_1: T2D vs. CON; p_2: T2D vs. MET; p_3: MET vs. CON; F: Statistic of single-factor analysis of variance; p: Significance level of single-factor analysis of variance.

to the CON group. In the MET group, FBG (p = 0.026) was significantly lower than that in the T2D group. Additionally, FBG (p = 0.032) and HbA1c (p = 0.000) in the MET group were significantly higher than those in the CON group. Other observed changes were not statistically significant. Indicators of kidney function, such as lood urea nitrogen (BUN) and Creatinine (CREA), were within normal ranges.

Standard Curve and Chromatographic Separation Effect

Regression analysis was conducted using the least square method, and the calibration solution recovery (accuracy) and correlation coefficient (R2) yielded optimal results when the weight was set to 1/x (refer to **Supplementary File 6** for the standard curves of 56 compounds). The absolute content of metabolites was analyzed in MRM-mode using MultiQuant 3.0.3 software. In this analysis, the method employed in detection ensured that all target compounds exhibited symmetrical chromatographic peaks, and effective chromatographic separation of each target compound was achieved. There were no significant differences observed in the retention time and chromatographic peak shape of the target compounds between the biological samples and the standard solution (**Supplementary File 7**).

Methodological Validation and Multivariate Statistical Analysis

Methodological validation, as presented in **Supplementary Files 8,9**, demonstrated that the experimental method can accurately detect the content of target metabolites in the samples. Upon obtaining the quantitative expression matrix of metabolites, PCA was initially performed. PCA, a statistical method, transforms a set of potentially correlated variables into linear uncorrelated variables (principal components) through orthogonal transformation [40]. However, in this experiment, PCA analysis did not effectively distinguish the three groups. Consequently, ropls R package was employed for OPLS-DA instead of PCA analysis [41].

Through OPLS-DA analysis, orthogonal variables unrelated to categorical variables in metabolites were filtered out. Non-orthogonal variables and orthogonal variables were analyzed separately to extract more reliable information regarding inter-group differences in metabolites and the correlation degree of the experimental groups [42]. In Fig. 1A, the two groups of samples were significantly distinguished, and all samples fell within a 95% confidence interval (Hotelling's T-squared ellipse). In Fig. 1B, the slopes of the two dashed lines were positive, and all the green dots were above the blue dots, indicating the validity of the OPLS-DA model. Fig. 1C further confirmed the model's optimal status, with Q2 = 0.564 $>$ 0.5 and R2Y = 0.659 $>$ 0.5 (Q2 $>$ 0.5 and R2Y $>$ 0.5 are the goodness-of-fit and predictive ability parameters, respectively) [43,44], and p $<$ 0.05.

As the OPLS-DA model construction for T2D vs. CON ($p > 0.05$) and MET vs. CON ($p > 0.05$) was unsuccessful (refer to **Supplementary Files 10,11**), only a student t-test and fold change analysis were conducted for T2D vs. CON and MET vs. CON, without multivariate statistical analysis and visual display.

Differential Metabolite Screening

The student t-test, a univariate statistical method with a significance threshold of $p < 0.05$, was employed. This

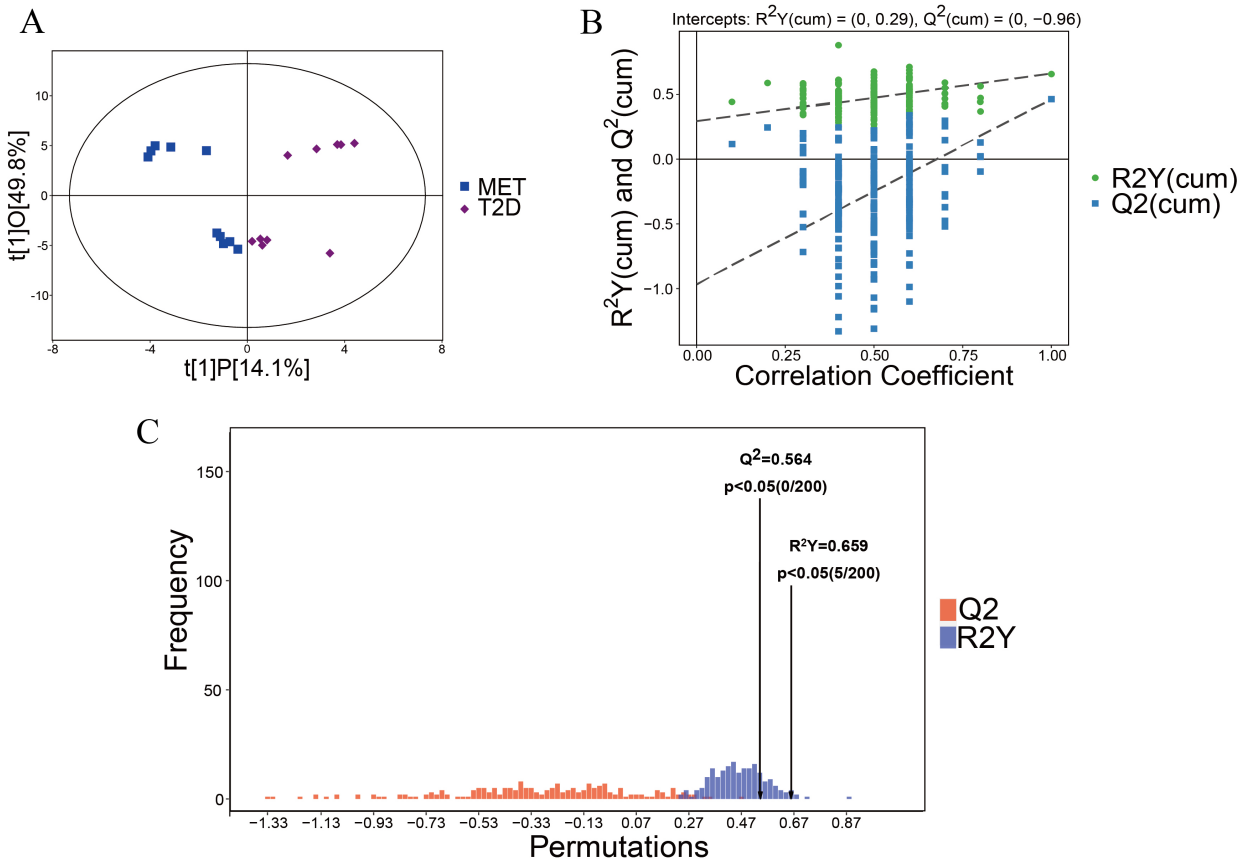

Fig. 1. Analysis of OPLS-DA in MET vs. T2D. (A) OPLS-DA scatter plot. The horizontal coordinate t[1]P showed the differences between sample groups, and the vertical coordinate t[1]O showed the differences within sample groups. Each scatter point represented a sample, and the scatter shape and color represented different experimental groups. (B) OPLS-DA permutation test diagram. The horizontal coordinate represented the permutation retention, the vertical coordinate represents the RY or Q value, the green dot represented the RY value obtained by the permutation test, the blue square dot represented the Q value obtained by the permutation test, and the two dashed lines represented the regression line of RY and Q, respectively. It was generally believed that the slope of the fitted regression line was positive and all green dots were above the blue dots, indicating that there was no overfitting and the model was valid. (C) OPLS-DA permutation test bar chart. The horizontal coordinate represented the accuracy of the random model of permutation test, the vertical coordinate represented the number of random models, the red bar chart represented the number of occurrences of Q2 value obtained by permutation test, and the blue bar chart represented the number of occurrences of R2Y value obtained by permutation test. It was generally accepted that $p < 0.05$, the model was optimal. OPLS-DA, Orthogonal Partial Least Squares Discriminant Analysis.

analysis resulted in the identification of 7 metabolites for T2D vs. CON and 9 metabolites for MET vs. T2D. Utilizing the online Venn diagram tool (version 2.1.0, https://bioinfogp.cnb.csic.es/tools/venny/index.html), a Venn figure was generated (Fig. 2A), revealing that T2D vs. CON and MET vs. T2D shared five common differential metabolites. Subsequently, a volcano plot was constructed using R ggplot2 (Fig. 2B), which screened nine differential metabolites.

Table 2 comprehensively summarizes the changes in all differential metabolites before and after metformin therapy for T2DM. Notably, cyclic 3′,5′-AMP, glucose 6-phosphate, L-lactic acid, malic acid, and maleic acid exhibited opposite changes before and after metformin treatment for T2DM ($p < 0.05$).

Differential Metabolite Correlation Analysis

Correlation analysis of metabolites is instrumental in gaining a deeper understanding of the mutual regulatory relationships and synergistic changes between metabolites during biological state transitions. For each group comparison, correlation coefficients of quantitative metabolite values were calculated using the Pearson method and presented in the form of heatmaps [45]. Fig. 3 illustrates that L-lactic acid exhibited a positive correlation with malic acid ($r = 0.94$, $p < 0.05$), as did malic acid with maleic acid ($r = 0.82$, $p < 0.05$), and malic acid with succinic acid ($r = 0.81$, $p < 0.05$). Moreover, other metabolites examined for metformin reversal also displayed positive associations, such as L-lactic acid with succinic acid ($r = 0.78$, $p < 0.05$), and L-lactic acid with glucose-6-phosphate ($r = 0.72$, $p < 0.05$).

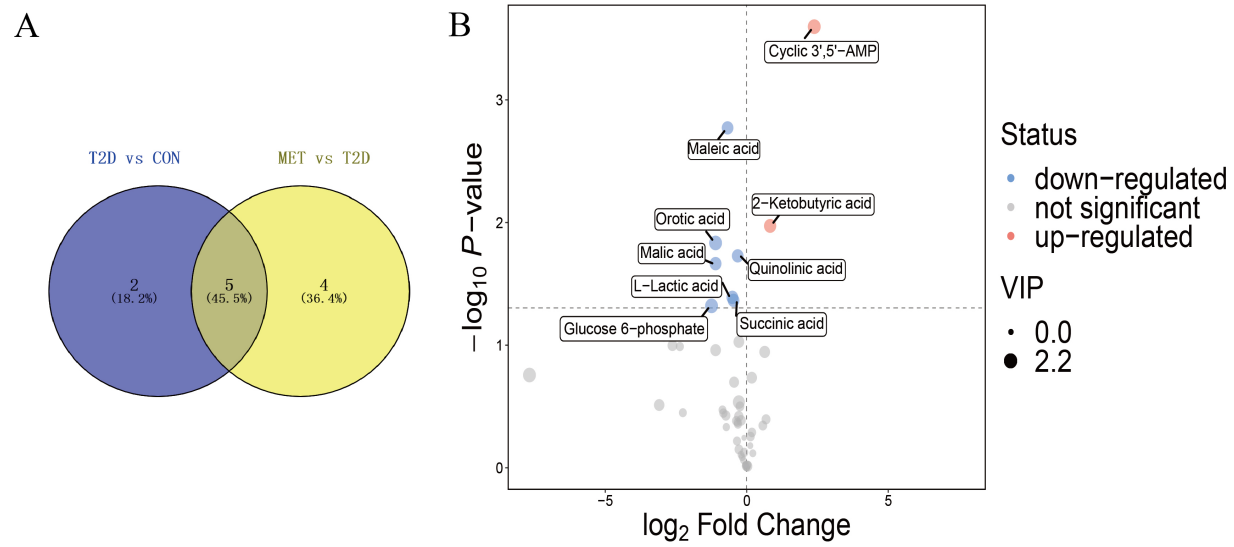

Fig. 2. Differential metabolite screening. (A) T2D vs. CON and MET vs. T2D Venn diagram. The purple circle represented the differential metabolite of T2D vs. CON, the yellow circle represented the differential metabolite of MET vs. T2D, and the part where the two circles intersect was the common differential metabolite of the two groups after comparison. (B) MET vs. T2D volcano maps. The volcano map was a combination of fold change (FC) and *t*-tests, with an X-axis of log2 (FC) and a Y-axis of –log10 (*p*-value), with red dots for up and blue dots for down. Each dot in the figure represented a metabolite, and the size of the dot represented the variable importance in the projection (VIP) value of the OPLS-DA model. The larger the dot, the larger the VIP value, and the more reliable the differentially expressed metabolites obtained by screening. $p < 0.05$.

These metabolites, exhibiting significant correlations, may potentially participate in the same metabolic pathway, offering valuable insights for the identification of therapeutic targets for T2D.

Analysis of Metabolic Pathways of Differential Metabolites

We utilized the online analytical tools of MetaboAnalyst 5.0 (https://www.metaboanalyst.ca/MetaboAnalyst/upload/PathUploadView.xhtml) for a comprehensive analysis of differential metabolites through pathway enrichment analysis and topology analysis. This approach aids in identifying key pathways with the highest correlation to metabolite differences [46]. Fig. 4 illustrates the results, highlighting that Citrate cycle (TCA cycle), Glycolysis or Gluconeogenesis, Propanoate metabolism, and Pyruvate metabolism were the four most enriched pathways ($p < 0.05$, FDR <0.2). Table 3 provides a summary of the enrichment information for metabolites in these four pathways. Subsequent studies could delve deeper into these metabolic pathways to unveil pathway-specific biomarkers and potential therapeutic targets.

Discussion

Over the past few decades, mass spectrometry has been employed not only for monitoring the efficacy of metformin [47–50] but also for delving into the molecular mechanisms underlying metformin's actions [51–53]. The HPIC-MS/MS method employed in this study enables the accurate quantification of 50 compounds related to CCM, with 6 compounds either not detected, below the detection limit, or missing data in each sample, resulting in rejection due to a threshold of >50%. The quantitative outcomes obtained through HPIC-MS/MS were subjected to univariate and multivariate statistical analyses. Subsequently, correlation and KEGG pathway analyses of the differential metabolites were conducted to ascertain the impact of metformin on the most relevant metabolic pathways within CCM.

In the newly diagnosed cases of T2D, five out of the seven differential metabolites exhibiting significant changes were reversed by metformin, returning to normal levels. Following metformin treatment for T2D, nine metabolites showed significant alterations, including five that were reversed. Notably, cyclic 3′,5′-AMP, glucose-6-phosphate, L-lactic acid, malic acid, maleic acid, and succinic acid were discussed to elucidate their clinical significance.

Cyclic 3′,5′-AMP serves as a signaling molecule mediating various processes, formed by the stimulation and activation of adenylate cyclase by certain hormones or other molecular signals. The levels of cyclic 3′,5′-AMP are influenced by cell metabolism [54]. Research has confirmed that cyclic 3′,5′-AMP plays a crucial role as a physiological amplifier for the secretion of glucose-induced insulin by islet β cells, particularly in response to the insulin-stimulating hormones GLP-1 (glucagon-like peptide-1) and GIP (glucose-dependent insulin-stimulating peptide) [55].

Table 2. Differential metabolites before and after metformin treatment of T2DM.

Differential metabolite	T2D vs. CON			MET vs. T2D			
	FC	*p* value	Regulated	FC	*p* value	VIP	Regulated
Cyclic 3′,5′-AMP	0.166	0.008	↓	5.21	0.000	2.15	↑
Maleic acid	1.662	0.002	↑	0.63	0.002	1.54	↓
Glucose 6-phosphate	3.156	0.021	↑	0.42	0.048	2.15	↓
L-Lactic acid	1.486	0.029	↑	0.70	0.041	1.61	↓
Malic acid	2.296	0.017	↑	0.47	0.022	1.60	↓
Ureidopropionic acid	0.792	0.035	↓				
Glyceric acid	1.922	0.001	↑				
2-Ketobutyric acid				1.77	0.011	1.78	↑
Orotic acid				0.47	0.015	2.12	↓
Quinolinic acid				0.80	0.019	1.51	↓
Succinic acid				0.72	0.043	1.55	↓

Note: FC, fold change; "↑", up-regulated; "↓", down-regulated. The *p*-value was obtained by *t*-test; VIP is obtained through OPLS-DA.

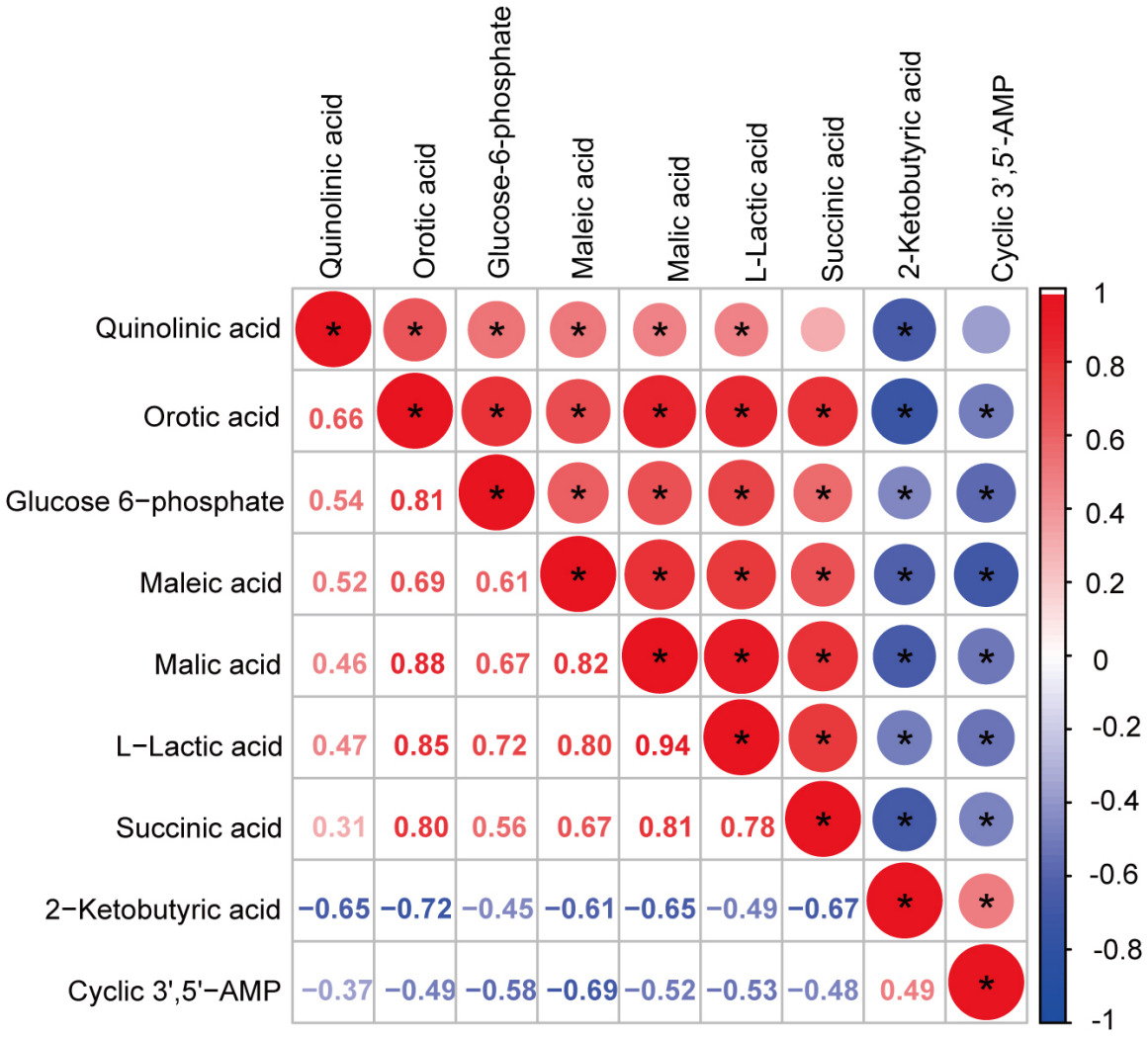

Fig. 3. Thermal maps of differential metabolite correlation analysis in the MET vs. T2D. The horizontal and vertical coordinated in the figure represented the metabolites in this group of comparison, and the color blocks at different positions represented the correlation coefficients between metabolites at corresponding positions. Red represented the positive correlation, blue represented the negative correlation, and the darker the color, the stronger the correlation. Significance correlations were marked with an * ($p < 0.05$).

Table 3. Four pathways of significant enrichment.

Pathway	Name	Metabolites	Raw *p*	FDR	Impact
ko00020	citrate cycle (TCA cycle)	succinic acid, malic acid	0.005	0.190	0.077
ko00620	pyruvate metabolism	L-lactic acid, malic acid	0.007	0.190	0.031
ko00640	propanoate metabolism	L-lactic, succinic acid	0.007	0.190	0.041
ko00010	glycolysis or gluconeogenesis	L-lactic acid, glucose-6-phosphate	0.009	0.190	0.029

Note: Raw *p* represented the *p*-value obtained by enrichment analysis; FDR represented the *p*-value corrected by multiple hypothesis tests using the false discovery rate method; impact indicated the impact factor obtained from topology analysis.

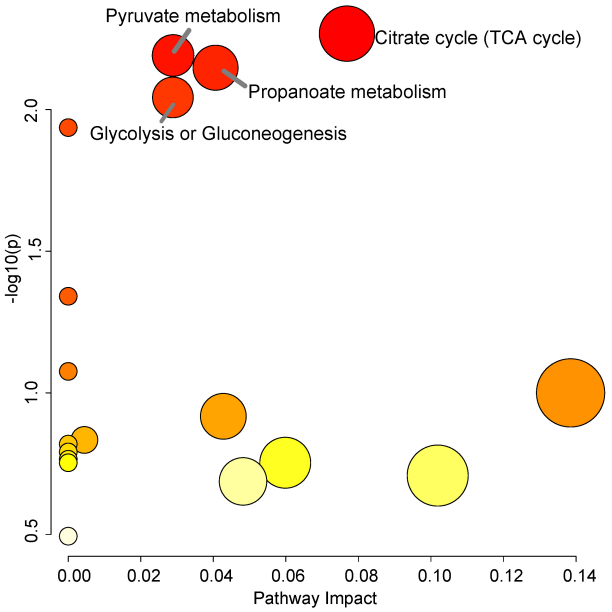

Fig. 4. Bubble maps of KEGG analysis in the MET vs. T2D group. In the bubble diagram, each bubble represented a metabolic pathway, and the horizontal coordinate where the bubble was located. The size of the bubble represented the influence factor of the pathway in topological analysis: The larger the bubble, the larger the influence factor. The vertical coordinate of the bubble and the color of the bubble represented the *p*-value of the enrichment analysis (take the negative natural logarithm, that is, –ln(p)). The darker the color, the smaller the *p*-value and the more significant the enrichment degree.

Raising the content of cyclic 3′,5′-AMP in beta cells may enhance insulin secretion. Our study revealed that metformin increased cyclic 3′,5′-AMP levels in serum, though whether it concurrently increased cyclic 3′,5′-AMP content in β cells requires further investigation.

Maleic acid, a cis-trans isomer of fumaric acid, acts differently from fumaric acid. Research indicates that maleic acid can interfere with mitochondrial oxidative metabolism in the kidney [56], potentially inducing proximal tubule dysfunction and injury [57]. Therefore, prolonged accumulation of maleic acid in the body may lead to significant kidney damage. Our study demonstrated that metformin reduced maleic acid levels in T2D, suggesting a potential reduction in the risk of kidney damage in individuals with T2D.

Glucose 6-phosphate serves as an intermediate metabolite in glycolysis/gluconeogenesis and the PPP. It plays a role in regulating the activity of glycogen synthase [58]. Hyperglycemia leads to elevated levels of glucose 6-phosphate in liver cells, skeletal muscle, and adipose tissue [59]. In our study, metformin reduced increased levels of glucose 6-phosphate in T2D, implying potential inhibition of CCM-related pathways such as glycolysis/gluconeogenesis and the PPP.

L-lactic acid, a product of anaerobic glycolysis, has been identified as an independent risk factor for T2D [60], significantly associated with the risk of developing T2D [61]. In our findings, L-lactic acid exhibited elevated levels in patients with newly diagnosed T2D, but decreased rather than increased, after treatment with metformin. This suggests that metformin may not elevate the potential risk of lactic acidosis in the early stages of T2D treatment (4–6 weeks) [62,63].

Malic acid and succinic acid, as intermediate metabolites of the TCA. Energy excess in T2D patients [64] may be related to TCA enhancement. Following metformin treatment, levels of malic acid and succinic acid decreased, indicating that metformin reduced the intermediates of the TCA. This observation aligns with the findings of Hohnholt's study [65]. In summary, we hypothesize that metformin weakens glycolysis and the TCA, leading to reduced ATP production and diminished energy accumulation. This effect may contribute to alleviating energy metabolism disorders in T2D.

Numerous studies have identified the pleiotropic effects of metformin [66,67]. It actively contributes to anti-aging [68], weight loss [69], cardiovascular protection [70], improvement of polycystic ovary syndrome [71], inhibition of tumors [72–74], anti-inflammatory properties [75], reversal of pulmonary fibrosis [76], reversal of cognitive dysfunction [77], and improvement of intestinal flora [78,79]. Virtually all of these effects are attributed to metformin's beneficial impact on metabolism. Therefore, metformin is perceived to enhance metabolism through multiple pathways [52,80–83].

The examination of clinical implications for the mentioned metabolites indicates that their levels largely decreased following metformin treatment. This observation suggests the possibility of mutual regulation and synergistic changes in different metabolic pathways involving these compounds. The significantly enriched metabolic pathways identified hold promise as potential therapeutic targets for metformin in T2D. However, further research is necessary to delve deeper into these pathways and confirm their therapeutic relevance.

Conclusions

In recent years, numerous publications have explored the mechanisms of metformin using metabolomics methods, yet the conclusions remain controversial. This study represents a novel application of HPIC-MS/MS targeted metabolomics in the serum of patients with T2D treated with metformin, offering valuable insights to elucidate the new mechanism through which metformin improves energy metabolism in T2D. Our findings indicate significant changes in the content of CCM in newly diagnosed T2D, suggesting that the disturbance of CCM may contribute to the development of T2D.

Metformin appears to primarily reduce CCM intermediates by influencing related metabolic pathways, such as the TCA, glycolysis or gluconeogenesis, pyruvate metabolism, and propanoate metabolism. Furthermore, we provide a reasonable explanation for the alterations in CCM metabolites, contributing to a deeper understanding of the mechanisms by which metformin improves energy metabolism. These insights may pave the way for more effective therapeutic applications of metformin.

Limitations

The small sample size and the limited number of metabolites obtained in this experiment can be considered as limitations. This study serves as a preliminary exploration, and subsequent efforts will involve an increase in sample size for validation purposes, as well as the inclusion of cell and animal experiments. The molecular mechanism underlying metformin's impact on CCM in newly diagnosed T2D patients will be further investigated through additional experiments, shedding light on changes in the glycolysis/gluconeogenesis, TCA and PPP. These endeavors aim to provide a more comprehensive understanding of the mechanism by which metformin negatively regulates CCM.

Availability of Data and Materials

Study data are included in this article or supplementary files, and further inquiries should be made to the corresponding author upon reasonable request.

Author Contributions

DX and QH designed the experiment. YS, LL, and WL completed the experiment. FY and LL analyzed and interpreted the data. YS, LL, and WL wrote the manuscript and plotted Figs. 1,2,3,4. QH, FY and DX put forward major suggestions for the revision of the article. Each author agrees to be responsible for the part they complete, ensuring the accuracy of each link. Each author reviewed the manuscript carefully, proposed his own revisions, and approved the final draft.

Ethics Approval and Consent to Participate

This study was approved by the Ethics Committee of the Hospital of Chengdu University of Traditional Chinese Medicine (Number: 2020KL-031). All study procedures were performed by the ethical standards of the institution/or National Research Council and under the Declaration of Helsinki of 1964. All participants who met the inclusion criteria received notification and signed informed consent.

Acknowledgment

Not applicable.

Funding

This study was supported by the Chengdu Science and Technology Bureau under Grant number 2021-YF05-01726-SN.

Conflict of Interest

The authors declare no conflict of interest.

Supplementary Material

Supplementary material associated with this article can be found, in the online version, at https://doi.org/10.24976/Discov.Med.202436183.64.

References

[1] Sun H, Saeedi P, Karuranga S, Pinkepank M, Ogurtsova K, Duncan BB, *et al*. IDF Diabetes Atlas: Global, regional and country-level diabetes prevalence estimates for 2021 and projections for 2045. Diabetes Research and Clinical Practice. 2022; 183: 109119.

[2] Zheng Y, Ley SH, Hu FB. Global aetiology and epidemiology of type 2 diabetes mellitus and its complications. Nature Reviews. Endocrinology. 2018; 14: 88–98.

[3] Chatterjee SKKDM. Type 2 diabetes. The Lancet. 2017; 389: 2192.

[4] Schernthaner G, Schernthaner GH. The right place for metformin today. Diabetes Research and Clinical Practice. 2020; 159: 107946.

[5] American Diabetes Association. Standards of medical care in diabetes–2008. Diabetes Care. 2008; 31: S12–S54.

[6] Nathan DM, Buse JB, Davidson MB, Heine RJ, Holman RR, Sherwin R, *et al*. Management of hyperglycemia in type 2 diabetes: A consensus algorithm for the initiation and adjustment of therapy: a consensus statement from the American Diabetes Association and the European Association for the Study of Diabetes. Diabetes Care. 2006; 29: 1963–1972.

[7] Diabetes Society of Chinese Medical Association. Guidelines for the prevention and treatment of type 2 diabetes in China (2020 edition). International Journal of Endocrinology and Metabolism. 2021; 41: 482–548.

[8] Andrzejewski S, Siegel PM, St-Pierre J. Metabolic Profiles Associated With Metformin Efficacy in Cancer. Frontiers in Endocrinology. 2018; 9: 372.

[9] Elgendy M, Cirò M, Hosseini A, Weiszmann J, Mazzarella L, Ferrari E, *et al*. Combination of Hypoglycemia and Metformin Impairs Tumor Metabolic Plasticity and Growth by Modulating the PP2A-GSK3β-MCL-1 Axis. Cancer Cell. 2019; 35: 798–815.e5.

[10] Li W, Chaudhari K, Shetty R, Winters A, Gao X, Hu Z, *et al*. Metformin Alters Locomotor and Cognitive Function and Brain Metabolism in Normoglycemic Mice. Aging and Disease. 2019; 10: 949–963.

[11] Rena G, Hardie DG, Pearson ER. The mechanisms of action of metformin. Diabetologia. 2017; 60: 1577–1585.

[12] Wang Y, An H, Liu T, Qin C, Sesaki H, Guo S, *et al*. Metformin Improves Mitochondrial Respiratory Activity through Activation of AMPK. Cell Reports. 2019; 29: 1511–1523.e5.

[13] Ma T, Tian X, Zhang B, Li M, Wang Y, Yang C, *et al*. Low-dose metformin targets the lysosomal AMPK pathway through PEN2. Nature. 2022; 603: 159–165.

[14] Xia H, Huang Z, Xu Y, Yam JWP, Cui Y. Reprogramming of central carbon metabolism in hepatocellular carcinoma. Biomedicine & Pharmacotherapy. 2022; 153: 113485.

[15] Hu C, Fan L, Cen P, Chen E, Jiang Z, Li L. Energy Metabolism Plays a Critical Role in Stem Cell Maintenance and Differentiation. International Journal of Molecular Sciences. 2016; 17: 253.

[16] Johnson CH, Ivanisevic J, Siuzdak G. Metabolomics: beyond biomarkers and towards mechanisms. Nature Reviews. Molecular Cell Biology. 2016; 17: 451–459.

[17] Roberts LD, Souza AL, Gerszten RE, Clish CB. Targeted metabolomics. Current Protocols in Molecular Biology. 2012; Chapter 30: Unit 30.2.1–Unit 30.2.24.

[18] Wang J, Christison TT, Misuno K, Lopez L, Huhmer AF, Huang Y, *et al*. Metabolomic profiling of anionic metabolites in head and neck cancer cells by capillary ion chromatography with Orbitrap mass spectrometry. Analytical Chemistry. 2014; 86: 5116–5124.

[19] Petucci C, Zelenin A, Culver JA, Gabriel M, Kirkbride K, Christison TT, *et al*. Use of Ion Chromatography/Mass Spectrometry for Targeted Metabolite Profiling of Polar Organic Acids. Analytical Chemistry. 2016; 88: 11799–11803.

[20] Devi S, Nongkhlaw B, Limesh M, Pasanna RM, Thomas T, Kuriyan R, *et al*. Acyl ethanolamides in Diabetes and Diabetic Nephropathy: Novel targets from untargeted plasma metabolomic profiles of South Asian Indian men. Scientific Reports. 2019; 9: 18117.

[21] Burzynska-Pedziwiatr I, Dudzik D, Sansone A, Malachowska B, Zieleniak A, Zurawska-Klis M, *et al*. Targeted and untargeted metabolomic approach for GDM diagnosis. Frontiers in Molecular Biosciences. 2023; 9: 997436.

[22] Li X, Li Y, Liang Y, Hu R, Xu W, Liu Y. Plasma Targeted Metabolomics Analysis for Amino Acids and Acylcarnitines in Patients with Prediabetes, Type 2 Diabetes Mellitus, and Diabetic Vascular Complications. Diabetes & Metabolism Journal. 2021; 45: 195–208.

[23] Hosseinkhani S, Arjmand B, Dilmaghani-Marand A, Mohammadi Fateh S, Dehghanbanadaki H, Najjar N, *et al*. Targeted metabolomics analysis of amino acids and acylcarnitines as risk markers for diabetes by LC-MS/MS technique. Scientific Reports. 2022; 12: 8418.

[24] Sun Y, Gao HY, Fan ZY, He Y, Yan YX. Metabolomics Signatures in Type 2 Diabetes: A Systematic Review and Integrative Analysis. The Journal of Clinical Endocrinology and Metabolism. 2020; 105: 1000–1008.

[25] Morze J, Wittenbecher C, Schwingshackl L, Danielewicz A, Rynkiewicz A, Hu FB, *et al*. Metabolomics and Type 2 Diabetes Risk: An Updated Systematic Review and Meta-analysis of Prospective Cohort Studies. Diabetes Care. 2022; 45: 1013–1024.

[26] Kim HW. Metabolomic Approaches to Investigate the Effect of Metformin: An Overview. International Journal of Molecular Sciences. 2021; 22: 10275.

[27] Agius L, Ford BE, Chachra SS. The Metformin Mechanism on Gluconeogenesis and AMPK Activation: The Metabolite Perspective. International Journal of Molecular Sciences. 2020; 21: 3240.

[28] LaMoia TE, Shulman GI. Cellular and Molecular Mechanisms of Metformin Action. Endocrine Reviews. 2021; 42: 77–96.

[29] Lv Z, Guo Y. Metformin and Its Benefits for Various Diseases. Frontiers in Endocrinology. 2020; 11: 191.

[30] Foretz M, Guigas B, Viollet B. Understanding the glucoregulatory mechanisms of metformin in type 2 diabetes mellitus. Nature Reviews. Endocrinology. 2019; 15: 569–589.

[31] Zabielski P, Hady HR, Chacinska M, Roszczyc K, Gorski J, Blachnio-Zabielska AU. The effect of high fat diet and metformin treatment on liver lipids accumulation and their impact on insulin action. Scientific Reports. 2018; 8: 7249.

[32] Ismail TA, Soliman MM, Nassan MA. Molecular and immunohistochemical effects of metformin in a rat model of type 2 diabetes mellitus. Experimental and Therapeutic Medicine. 2015; 9: 1921–1930.

[33] Classification and Diagnosis of Diabetes:Standards of Medical Care in Diabetes—2020. Diabetes Care. 2020; 43: S14–S31.

[34] World Medical Association. World Medical Association Declaration of Helsinki: ethical principles for medical research involving human subjects. JAMA. 2013; 310: 2191–2194.

[35] . Human Experimentation: Code of Ethics of the World Medical Association (Declaration of Helsinki). Canadian Medical Association Journal. 1964; 91: 619.

[36] Ou J, Peng Y, Yang W, Zhang Y, Hao J, Li F, *et al*. ABHD5 blunts the sensitivity of colorectal cancer to fluorouracil via promoting autophagic uracil yield. Nature Communications. 2019; 10: 1078.

[37] Yang K, Qiu T, Zhou J, Gong X, Zhang X, Lan Y, *et al*. Blockage of glycolysis by targeting PFKFB3 suppresses the development of infantile hemangioma. Journal of Translational Medicine. 2023; 21: 85.

[38] Dunn WB, Broadhurst D, Begley P, Zelena E, Francis-McIntyre S, Anderson N, *et al*. Procedures for large-scale metabolic profiling of serum and plasma using gas chromatography and liquid chromatography coupled to mass spectrometry. Nature Protocols. 2011; 6: 1060–1083.

[39] Saccenti E, Hoefsloot HCJ, Smilde AK, Westerhuis JA, Hendriks MM. Reflections on univariate and multivariate analysis of metabolomics data. Metabolomics. 2014; 10: 361–374.

[40] Ringnér M. What is principal component analysis? Nature Biotechnology. 2008; 26: 303–304.

[41] Thévenot EA, Roux A, Xu Y, Ezan E, Junot C. Analysis of the Human Adult Urinary Metabolome Variations with Age, Body Mass Index, and Gender by Implementing a Comprehensive Workflow for Univariate and OPLS Statistical Analyses. Journal

of Proteome Research. 2015; 14: 3322–3335.
[42] Worley B, Powers R. A Sequential Algorithm for Multiblock Orthogonal Projections to Latent Structures. Chemometrics and Intelligent Laboratory Systems. 2015; 149: 33–39.
[43] Peng C, Sun Z, Sun Y, Ma T, Li W, Zhang H. Characterization and association of bacterial communities and nonvolatile components in spontaneously fermented cow milk at different geographical distances. Journal of Dairy Science. 2021; 104: 2594–2605.
[44] Li Y, Quan H, Liang L, Yang T, Feng L, Mao X, *et al*. Non-targeted metabolomics reveals the discrimination of Cyclocarya paliurus leaves brewed by different methods. Food Research International. 2021; 142: 110221.
[45] Pawan, Dhiman R. Electroencephalogram channel selection based on pearson correlation coefficient for motor imagery-brain-computer interface. Measurement: Sensors. 2023; 25: 100616.
[46] Pang Z, Zhou G, Ewald J, Chang L, Hacariz O, Basu N, *et al*. Using MetaboAnalyst 5.0 for LC-HRMS spectra processing, multi-omics integration and covariate adjustment of global metabolomics data. Nature Protocols. 2022; 17: 1735–1761.
[47] Wattamwar T, Mungantiwar A, Halde S, Pandita N. Development of simultaneous determination of empagliflozin and metformin in human plasma using liquid chromatography-mass spectrometry and application to pharmacokinetics. European Journal of Mass Spectrometry. 2020; 26: 117–130.
[48] Strugaru AM, Kazakova J, Butnaru E, Caba IC, Bello-López MÁ, Fernández-Torres R. Simultaneous determination of metformin and glimepiride in human serum by ultra high performance liquid chromatography quadrupole time of flight mass spectrometry detection. Journal of Pharmaceutical and Biomedical Analysis. 2019; 165: 276–283.
[49] Antonopoulos N, Machairas G, Migias G, Vonaparti A, Brakoulia V, Pistos C, *et al*. Hydrophilic Interaction Liquid Chromatography-Electrospray Ionization Mass Spectrometry for Therapeutic Drug Monitoring of Metformin and Rosuvastatin in Human Plasma. Molecules. 2018; 23: 1548.
[50] Shah PA, Shah JV, Sanyal M, Shrivastav PS. LC-tandem mass spectrometry method for the simultaneous determination of metformin and sitagliptin in human plasma after ion-pair solid phase extraction. Journal of Pharmaceutical and Biomedical Analysis. 2016; 131: 64–70.
[51] Zhao H, Lyu Y, Zhai R, Sun G, Ding X. Metformin Mitigates Sepsis-Related Neuroinflammation *via* Modulating Gut Microbiota and Metabolites. Frontiers in Immunology. 2022; 13: 797312.
[52] Dahabiyeh LA, Mujammami M, AlMalki RH, Arafat T, Benabdelkamel H, Alfadda AA, *et al*. Lipids Alterations Associated with Metformin in Healthy Subjects: An Investigation Using Mass Spectrometry Shotgun Approach. International Journal of Molecular Sciences. 2022; 23: 11478.
[53] Tarry-Adkins JL, Robinson IG, Reynolds RM, Aye ILMH, Charnock-Jones DS, Jenkins B, *et al*. Impact of Metformin Treatment on Human Placental Energy Production and Oxidative Stress. Frontiers in Cell and Developmental Biology. 2022; 10: 935403.
[54] Kim HS, Kim SM, Lee HJ, Park SJ, Lee KH. Expression of the cpdA gene, encoding a 3′,5′-cyclic AMP (cAMP) phosphodiesterase, is positively regulated by the cAMP-cAMP receptor protein complex. Journal of Bacteriology. 2009; 191: 922–930.
[55] Furman B, Pyne N, Flatt P, O'Harte F. Targeting beta-cell cyclic 3′5′ adenosine monophosphate for the development of novel drugs for treating type 2 diabetes mellitus. A review. The Journal of Pharmacy and Pharmacology. 2004; 56: 1477–1492.
[56] Roginski AC, Cecatto C, Wajner SM, Camera FD, Castilho RF, Wajner M, *et al*. Experimental evidence that maleic acid markedly compromises glutamate oxidation through inhibition of glutamate dehydrogenase and α-ketoglutarate dehydrogenase activities in kidney of developing rats. Molecular and Cellular Biochemistry. 2019; 458: 99–112.
[57] Tuncel AT, Ruppert T, Wang BT, Okun JG, Kölker S, Morath MA, *et al*. Maleic Acid–but Not Structurally Related Methylmalonic Acid–Interrupts Energy Metabolism by Impaired Calcium Homeostasis. PLoS ONE. 2015; 10: e0128770.
[58] McCorvie TJ, Loria PM, Tu M, Han S, Shrestha L, Froese DS, *et al*. Molecular basis for the regulation of human glycogen synthase by phosphorylation and glucose-6-phosphate. Nature Structural & Molecular Biology. 2022; 29: 628–638.
[59] Villar-Palasí C, Guinovart JJ. The role of glucose 6-phosphate in the control of glycogen synthase. FASEB Journal. 1997; 11: 544–558.
[60] Juraschek SP, Shantha GPS, Chu AY, Miller ER, 3rd, Guallar E, Hoogeveen RC, *et al*. Lactate and risk of incident diabetes in a case-cohort of the atherosclerosis risk in communities (ARIC) study. PLoS ONE. 2013; 8: e55113.
[61] Guasch-Ferré M, Santos JL, Martínez-González MA, Clish CB, Razquin C, Wang D, *et al*. Glycolysis/gluconeogenesis- and tricarboxylic acid cycle-related metabolites, Mediterranean diet, and type 2 diabetes. The American Journal of Clinical Nutrition. 2020; 111: 835–844.
[62] Cayley WE, Jr. Does metformin increase the risk of fatal or nonfatal lactic acidosis? American Family Physician. 2010; 82: 1068–1070.
[63] Salpeter SR, Greyber E, Pasternak GA, Salpeter Posthumous EE. Risk of fatal and nonfatal lactic acidosis with metformin use in type 2 diabetes mellitus. The Cochrane Database of Systematic Reviews. 2010; CD002967.
[64] Ji L, Hu D, Pan C, Weng J, Huo Y, Ma C, *et al*. Primacy of the 3B approach to control risk factors for cardiovascular disease in type 2 diabetes patients. The American Journal of Medicine. 2013; 126: 925.e11–925.e22.
[65] Hohnholt MC, Blumrich EM, Waagepetersen HS, Dringen R. The antidiabetic drug metformin decreases mitochondrial respiration and tricarboxylic acid cycle activity in cultured primary rat astrocytes. Journal of Neuroscience Research. 2017; 95: 2307–2320.
[66] Rojas LBA, Gomes MB. Metformin: an old but still the best treatment for type 2 diabetes. Diabetology & Metabolic Syndrome. 2013; 5: 6.
[67] Cani PD. Human gut microbiome: hopes, threats and promises. Gut. 2018; 67: 1716–1725.
[68] Soukas AA, Hao H, Wu L. Metformin as Anti-Aging Therapy: Is It for Everyone? Trends in Endocrinology and Metabolism. 2019; 30: 745–755.
[69] Yerevanian A, Soukas AA. Metformin: Mechanisms in Human Obesity and Weight Loss. Current Obesity Reports. 2019; 8: 156–164.
[70] Nesti L, Natali A. Metformin effects on the heart and the cardiovascular system: A review of experimental and clinical data. Nutrition, Metabolism, and Cardiovascular Diseases. 2017; 27: 657–669.
[71] Yen H, Chang YT, Yee FJ, Huang YC. Metformin Therapy for Acne in Patients with Polycystic Ovary Syndrome: A Systematic Review and Meta-analysis. American Journal of Clinical Dermatology. 2021; 22: 11–23.
[72] Wheaton WW, Weinberg SE, Hamanaka RB, Soberanes S, Sullivan LB, Anso E, *et al*. Metformin inhibits mitochondrial complex I of cancer cells to reduce tumorigenesis. eLife. 2014; 3: e02242.
[73] Mallik R, Chowdhury TA. Metformin in cancer. Diabetes Research and Clinical Practice. 2018; 143: 409–419.
[74] Morales DR, Morris AD. Metformin in cancer treatment and pre-

vention. Annual Review of Medicine. 2015; 66: 17–29.
[75] Bharath LP, Nikolajczyk BS. The intersection of metformin and inflammation. American Journal of Physiology. Cell Physiology. 2021; 320: C873–C879.
[76] Cheng D, Xu Q, Wang Y, Li G, Sun W, Ma D, *et al*. Metformin attenuates silica-induced pulmonary fibrosis via AMPK signaling. Journal of Translational Medicine. 2021; 19: 349.
[77] Liao W, Xu J, Li B, Ruan Y, Li T, Liu J. Deciphering the Roles of Metformin in Alzheimer's Disease: A Snapshot. Frontiers in Pharmacology. 2022; 12: 728315.
[78] Weersma RK, Zhernakova A, Fu J. Interaction between drugs and the gut microbiome. Gut. 2020; 69: 1510–1519.
[79] Vallianou NG, Stratigou T, Tsagarakis S. Metformin and gut microbiota: their interactions and their impact on diabetes. Hormones. 2019; 18: 141–144.
[80] He L. Metformin and Systemic Metabolism. Trends in Pharmacological Sciences. 2020; 41: 868–881.
[81] Adam J, Brandmaier S, Leonhardt J, Scheerer MF, Mohney RP, Xu T, *et al*. Metformin Effect on Nontargeted Metabolite Profiles in Patients With Type 2 Diabetes and in Multiple Murine Tissues. Diabetes. 2016; 65: 3776–3785.
[82] Song Y, Liu Z, Zhu X, Hao C, Hao W, Wu S, *et al*. Metformin alleviates the cognitive impairment caused by aluminum by improving energy metabolism disorders in mice. Biochemical Pharmacology. 2022; 202: 115140.
[83] Tokubuchi I, Tajiri Y, Iwata S, Hara K, Wada N, Hashinaga T, *et al*. Beneficial effects of metformin on energy metabolism and visceral fat volume through a possible mechanism of fatty acid oxidation in human subjects and rats. PLoS ONE. 2017; 12: e0171293.